esa ECOSPHERE

ECOLOGY OF CRITICAL ZONES

Spatiotemporal variability of gas transfer velocity in a tropical high-elevation stream using two independent methods

Keridwen M. Whitmore,[1] Nehemiah Stewart,[2] Andrea C. Encalada,[3] Esteban Suárez,[3] and Diego A. Riveros-Iregui[1,†]

[1]Department of Geography, University of North Carolina at Chapel Hill, Chapel Hill, North Carolina 27599 USA
[2]Department of Chemistry, University of North Carolina at Chapel Hill, Chapel Hill, North Carolina 27599 USA
[3]Laboratorio de Ecología Acuática, Instituto BIOSFERA, Universidad San Francisco de Quito, Quito, Ecuador

Citation: Whitmore, K. M., N. Stewart, A. C. Encalada, E. Suárez, and D. A. Riveros-Iregui. 2021. Spatiotemporal variability of gas transfer velocity in a tropical high-elevation stream using two independent methods. Ecosphere 12(7): e03647. 10.1002/ecs2.3647

Abstract. Streams in high-elevation tropical ecosystems known as páramos may be significant sources of carbon dioxide (CO_2) to the atmosphere by transforming terrestrial carbon to gaseous CO_2. Studies of these environments are scarce, and estimates of CO_2 fluxes are poorly constrained. In this study, we use two independent methods for measuring gas transfer velocity (k), a critical variable in the estimation of CO_2 evasion and other biogeochemical processes. The first method, kinematic k_{600} ($k_{600\text{-K}}$), is derived from an empirical relationship between temperature-adjusted k (k_{600}) and the physical characteristics of the stream. The second method, measured k_{600} ($k_{600\text{-M}}$), estimates gas transfer velocity in the stream by in situ measurements of dissolved CO_2 (pCO_2) and CO_2 evasion to the atmosphere, adjusting for temperature. Measurements were collected throughout a 5-week period during the wet season of a peatland-stream transition within a páramo ecosystem located above 4000 m in elevation in northeastern Ecuador. We characterized the spatial heterogeneity of the 250-m reach on five occasions, and both methods showed a wide range of variability in k_{600} at small spatial scales. Values of $k_{600\text{-K}}$ ranged from 7.42 to 330 m/d (mean = 116 ± 95.1 m/d), whereas values of $k_{600\text{-M}}$ ranged from 23.5 to 444 m/d (mean = 121 ± 127 m/d). Temporal variability in k_{600} was driven by increases in stream discharge caused by rain events, whereas spatial variability was driven by channel morphology, including stream width and slope. The two methods were in good agreement (less than 16% difference) at high and medium stream discharge (above 7.0 L/s). However, the two methods considerably differed from one another (up to 73% difference) at low stream discharge (below 7.0 L/s, which represents 60% of the observations collected). Our study provides the first estimates of k_{600} values in a high-elevation tropical catchment across steep environmental gradients and highlights the combined effects of hydrology and stream morphology in co-regulating gas transfer velocities in páramo streams.

Key words: carbon budget; CO_2 evasion; gas transfer velocity; high elevation; mountain streams; topical páramo.

Received 31 August 2020; revised 19 February 2021; accepted 5 March 2021; final version received 11 May 2021. Corresponding Editor: Rebecca Titus Barnes.

† **E-mail:** diegori@unc.edu

Introduction

A growing body of work highlights the important role that rivers play in the transformation of terrestrial carbon and stream organic matter to atmospheric CO_2 (Johnson et al. 2008, Battin et al. 2009, Aufdenkampe et al. 2011). Rivers have been found to return half of the carbon they receive from the landscape to the atmosphere (Cole et al. 2007), with global estimates of CO_2 evasion ranging from 650 to 1800 Tg C/yr (Benstead and Leigh 2012, Raymond et al. 2013, Lauerwald et al. 2015). Headwater streams contribute an outsized proportion of CO_2 emissions from lotic environments owing to their greater contact with both the atmosphere and benthic substrates, and higher turbulence than larger rivers (Downing et al. 2012, Hotchkiss et al. 2015, Schelker et al. 2016).

While CO_2 evasion from rivers is a significant component of the global carbon budget, evasion estimates remain poorly constrained, particularly in headwater streams where direct measurements are challenging due to steep gradients, high water velocities, and heterogeneous channel geomorphology (Schelker et al. 2016, Horgby et al. 2019, Ulseth et al. 2019). A key variable in the estimation of CO_2 evasion is gas transfer velocity (k), which incorporates solubility of CO_2 in water and is often rate-limiting for gas fluxes (Zappa et al. 2007). Accurate estimates of k are needed to estimate CO_2 evasion as well as other biogeochemical processes such as carbon (C) storage, stream metabolism, and denitrification (Marzolf et al. 1994, McCutchan et al. 1998, Bott 2007). Selecting an appropriate k value is critical when upscaling biogeochemical processes observed at small scales (e.g., stream reaches) to an entire riverscape (Raymond et al. 2012).

Recently, mountainous streams have shown surprisingly high rates of evasion due to characteristically high turbulence (Horgby et al. 2019). Tropical mountainous streams are believed to have higher CO_2 evasion than their temperate counterparts (Aufdenkampe et al. 2011, Horgby et al. 2019) owing to the high rates of ecosystem C storage in soils and surrounding peatlands (e.g., Hribljan et al. 2017) combined with high rates of precipitation (Food and Agriculture Organization of the United Nations 2003). Furthermore, concentration of dissolved CO_2 and annual precipitation is correlated with CO_2 evasion (Butman and Raymond 2011). A recent study directly measured CO_2 evasion of a headwater stream of the Ecuadorian Andes and found CO_2 evasion to be greater than evasion from wetlands and rivers at lower elevation in the central Amazon (Schneider et al. 2020). Despite the potentially high rates of evasion from tropical mountains, studies of CO_2 evasion from small streams remain limited in the Tropical Andes, particularly at the highest elevations (Riveros-Iregui et al. 2018). Measurements of k and factors controlling its variability in these streams are absent from current literature, limiting our understanding of the fate of terrestrial C and hindering our ability to incorporate these ecosystems into global C budgets.

The goal of this study was to characterize the spatiotemporal dynamics of k in a small, high-altitude peatland stream in Ecuador. We used two independent methods for estimating k. The first method was termed kinematic k ($k_{600\text{-K}}$), based on an empirically derived relationship between k_{600} and kinematic properties of the stream (Raymond et al. 2012). The second method was termed measured k ($k_{600\text{-M}}$) and was calculated by combining direct measurements of dissolved CO_2 (pCO_2) with direct measurements of CO_2 evasion at the water surface (McDowell and Johnson 2018), and scaling to the Schmidt number of 600 that corresponds to CO_2 at 20°C (k_{600}; Wanninkhof 2014). Both methods were used to examine spatial and temporal variability of gas transfer velocity along a 250-m study reach over a 5-week period. This information provides much-needed characterization of factors influencing CO_2 evasion in tropical mountainous streams.

Methods

Site description

Our study was located within the páramo ecoregion of the northeastern Andean mountains. A tropical alpine ecosystem, the páramo, ranges in elevation from approximately 3500 to 4500 m and extends from Venezuela to northern Perú, discontinuously covering 36,000 km^2 (Mena Vásconez and Medina 2001). High rates of precipitation coupled with U-shaped valleys carved by past glacial activity form pools, swamps, and peatlands throughout páramo ecosystems (Josse et al. 2009).

Data for this study were collected from a small peatland stream within the Cayambe Coca National Park, 33 km east of Quito, Ecuador. The páramo ecosystem at the National Park has a mean daily temperature of 5°C and an annual precipitation of 1375 mm (Sánchez et al. 2017).

Elevation of the headwater catchment ranged from approximately 4090 to 4410 m. Our study stream reach, located at the base of the catchment, drains a 2.3-ha wetland and represents the first 250 m of the stream channel (Fig. 1). Field measurements were collected at the beginning of the wet season in this part of the Ecuadorian páramos (Sklenář and Lægaard 2003) and extended for five weeks. Precipitation records dating back to 2012 were provided by a nearby weather station, maintained by the Fondo para la Protección del Agua Network (FONAG; Station No. M5025, latitude −0.33, longitude −78.19).

Study design

In this study, we characterized gas transfer velocity, adjusted to a Schmidt number of 600, both temporally and spatially using two independent methods, which are described in detail below. Temporal dynamics of $k_{600\text{-M}}$ were

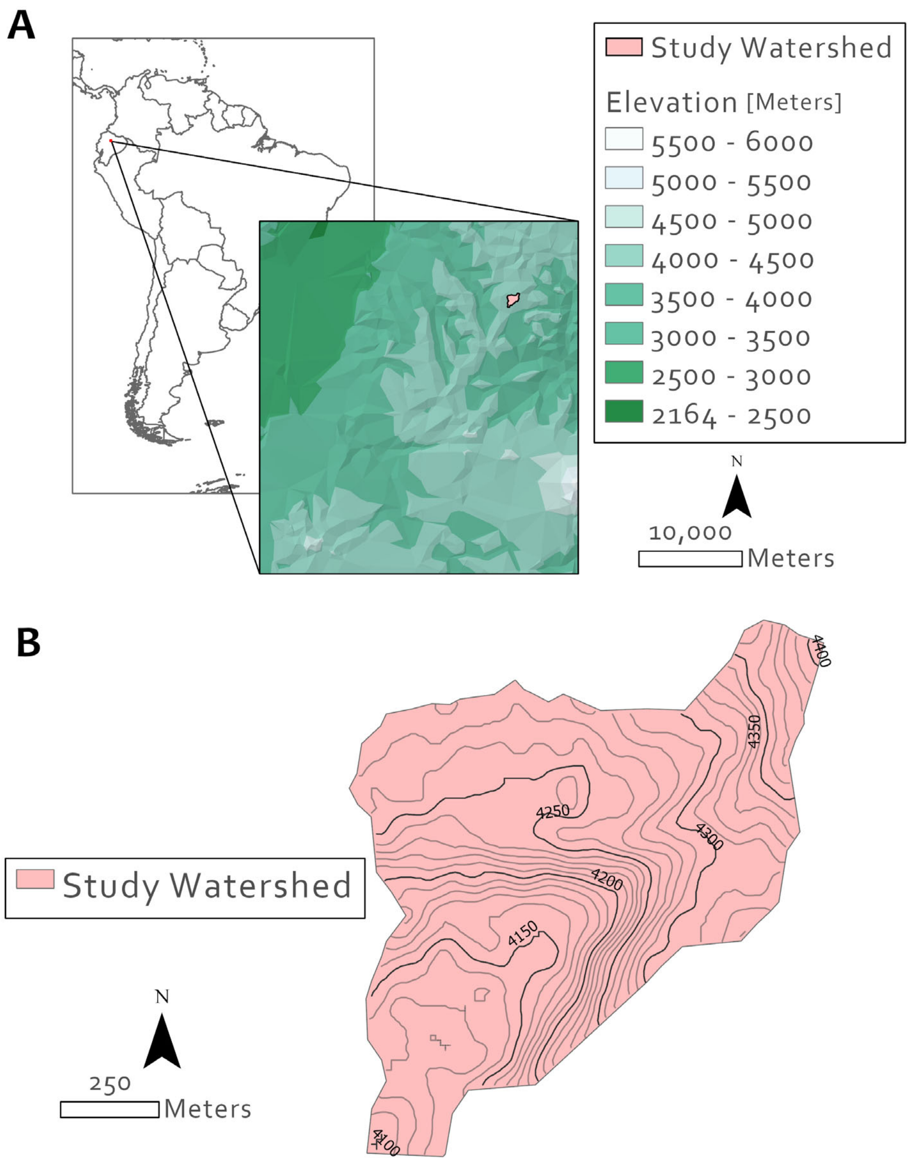

Fig. 1. (A) Location of Cayambe Coca Ecological Reserve, Ecuador. (B) Delineation of our study catchment within the reserve.

characterized by collecting measurements of partial pressure of CO_2 (pCO_2) and CO_2 evasion continuously, within 20 m from the peatland outlet, from 10 July to 18 August 2019. Depth, velocity, and slope measurements for calculating $k_{600\text{-}K}$ were collected in the same section of stream 16 times during the same period. Spatial dynamics of $k_{600\text{-}M}$ and $k_{600\text{-}K}$ were characterized by collecting data every six to seven days, for a total of five times, at regular intervals along the stream and between 1000 and 1600 local time (LT). Measurements for $k_{600\text{-}K}$ were collected at 34 locations, and measurements for $k_{600\text{-}M}$ were collected at 10 locations along the 250-m study reach (Fig. 2).

Gas transfer velocity calculations

$k_{600\text{-}K}$ was calculated using a previously developed relationship, commonly used in 1st-order streams (Raymond et al. 2012; Eq. 1). This equation involves the kinematic properties of the location, including water velocity (V, in m/s), depth (D, in m) and slope (S, unitless), and their observed effects on $k_{600\text{-}K}$ values.

$$k_{600-K} = (V \times D)^{0.089} \times D^{0.054} \times 5037 \quad (1)$$

$k_{600\text{-}M}$ was adapted from McDowell and Johnson (2018) and based on Henry's Law of solubility and Fick's first law of diffusion (Eq. 2) and converted to a Schmidt number of 600 (Eq. 3). Fick's first law of diffusion describes gaseous evasion from ter to the atmosphere, in which flux is a product of the gas transfer velocity and the CO_2 concentration gradient between water and air:

$$k = \frac{F_{CO_2}}{(C_w - C_{air}) \times K_H} \quad (2)$$

$$k_{600-M} = k \times \left(\frac{600}{Sc_{CO_2}}\right)^{-0.5} \quad (3)$$

Gas transfer velocity (k in m/d) is equal to the flux of CO_2 divided by the product of the concentration gradient of CO_2 between water and air and Henry's Law constant adjusted to the temperature of the stream (K_H in mol·m^{-3}·atm^{-1}; Eq. 2). Flux was measured directly as described in *Instrumentation* and converted to appropriate units (F_{CO2} in g C-CO_2·m^{-2}·d^{-1}). Partial pressure of CO_2 measured by infrared gas analyzer (IRGA) sensors was converted to mass concentration of dissolved C as CO_2 in the water (C_w in g C-CO_2/m^3) using Henry's law (Raymond et al. 2012). Atmospheric CO_2 was assumed to be 410 ppm based on the global average atmospheric CO_2 measurement collected in dry air by Mauna Loa Observatory during our study period (NOAA ESRL Global Monitoring Laboratory 2019). Water vapor was accounted for by subtracting partial pressure of water (assumed to be 100% humidity at the water/air interface) from barometric pressure. We used the ideal gas law

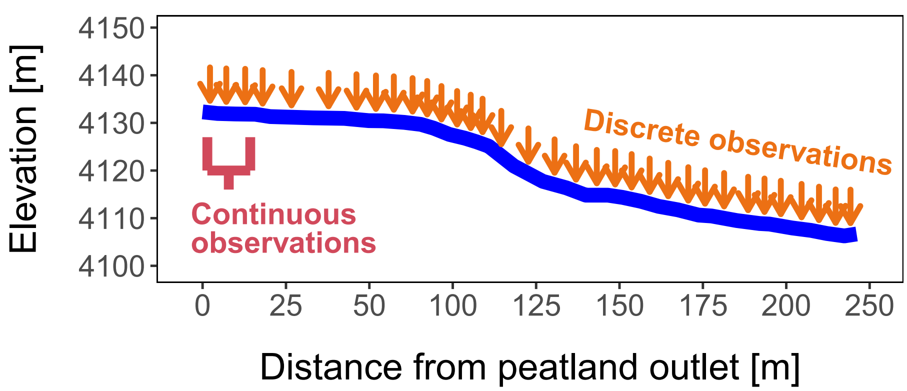

Fig. 2. Topographic stream profile of the study reach in the Cayambe Coca National Park. Illustrated are the stream sub-reach where continuous observations were collected (red bracket) during the 5-week study period, and the locations of 34 discrete observations (orange arrows) collected throughout the 250-m stream reach on five different occasions. Measurements of pCO_2, velocity, depth, and slope were collected from all locations. Measurements of CO_2 evasion were collected within sub-reach and at a subset of 10 discrete locations distributed throughout the stream reach. A 4-m waterfall was located 107 m downstream from the peatland outlet. The ratio of y-axis to x-axis is 2:1 to highlight elevation change.

to find the concentration of CO_2 (C_{air} in g C-CO_2/m^3). $k_{600\text{-}M}$ (m/d) was calculated as the product of the gas transfer velocity in m/d and 600 over Schmidt number for CO_2 at stream temperature. Because the Schmidt number's exponent may vary from −0.5 to −0.667, we selected the exponent −0.5 to reflect the turbulent surface of a lotic environment (Eq. 3; Jähne et al. 1987, Wanninkhof 2014).

We evaluated the potential effects introduced by the assumed atmospheric CO_2 concentration by testing the sensitivity of CO_2 evasion to changes in C_{air} and calculating $k_{600\text{-}M}$ at three different values, ranging 200 ppm (310, 410, and 510). Our analysis revealed that the percent difference in $k_{600\text{-}M}$ values never exceeded 5%, suggesting that the assumed atmospheric CO_2 values do not compromise calculation of CO_2 evasion. For the following analyses, the midrange value of 410 ppm was used.

Calculations, statistical analyses, and figures were completed using R software (RStudio, Boston, Massachusetts, USA). Data collected did not meet assumptions of normality, and therefore, non-parametric methods were used to complete statistical analysis. We applied a Mann-Whitney *U* test and Kruskal-Wallis test with post-hoc Dunn's pairwise using the Bonferroni adjustment.

Instrumentation

To calculate $k_{600\text{-}K}$, water velocity and depth were measured by water velocity probe (Model FP101, Global Flow Probe, Global Water, Gold River, California, USA) and wading rod, respectively. Stream-channel slope was determined remotely by collecting coordinates at midway points between synoptic sampling locations using a handheld GPS unit (Etrex 20x, Garmin, Olathe, Kansas, USA). A 3-m digital elevation model was collected using HD images by drone (Mavic Pro V1, DJI, Nanshan District, Shenzhen, China). Distance and elevation difference between each GPS locations was determined using ArcGIS pro software (ArcGIS Pro version 2.5.1, ESRI, Redland, California, USA, 2020).

We combined measurements of the partial pressure of dissolved CO_2 (pCO_2) with CO_2 evasion from the water surface to calculate $k_{600\text{-}M}$. Continuous pCO_2 was collected at 15-min intervals (GMP222 with transmitter, Vaisala, Helsinki, Finland) at two locations, 6.2 m and 140 m from the peatland outlet and logging to a datalogger (Bridge/Strain Gauge, Omega Engineering, Norwalk, Connecticut, USA). For synoptic sampling, we used a handheld CO_2 meter (GM70, Vaisala, Helsinki, Finland) set for the appropriate environmental pressure and allowed to stabilize for two to five min submerged in water and before recording a pCO_2 measurement. All solid-state sensors were adapted for wet environments as in Johnson et al. (2010), and all measurements were corrected following pressure and temperature compensatory procedures described by the manufacturer in the manual. Sensors were calibrated by manufacturer prior to deployment (accuracy = 1.5% of calibrated range [10,000 ppm] + 2% of reading). Once deployed, sensors were routinely checked against one another in the laboratory and the field, often using a third sensor, to ensure that outputs remained within the calibrated range and without drift throughout the study. Measurements were corrected for pressure and temperature using manufacturer reported equations. We did not observe a specific effect on equilibrium imposed by turbulence (e.g., lags, reading delays), likely because the observed variability in pCO_2 was larger than potential artifacts introduced by turbulence. In implementing our experimental design, we used these CO_2 sensors in the same way they have been used in previous studies (e.g., Crawford et al. 2013, Campeau et al. 2017, Tix et al. 2017, McDowell and Johnson 2018), many of them under turbulent conditions (e.g., Riveros-Iregui et al. 2018, Rocher-Ros et al. 2019). Our field observations confirmed what was originally reported by Johnson et al. (2010) in that it takes ~3 min for the sensor to reach equilibrium with dissolved CO_2 in the surrounding aquatic environment. Air pressure used for sensor compensation was measured using a barometric sensor (Model 3001, Solinst, Georgetown, Ontario, Canada) installed 17 m from the stream bank. Water temperature and additional pressure due to fluctuating water level were recorded by a water-level sensor (Model 3001, Solinst).

To measure CO_2 evasion from the water surface, we adapted two eosFD flux chambers (eosFD, Eosense, Dartmouth, Nova Scotia, Canada) with a floating platform as described by Schneider et al. (2020). Briefly, each eosFD flux chamber was placed on a floating platform constructed from a semi-rigid plastic disk with a diameter of 61 cm fastened to two pontoons made of 6.35 cm diameter PVC pipe. The pontoons were angled in a V configuration so that they would not create turbulent conditions prior to flow past the sensor. The semi-rigid plastic disk was fitted with a PVC collar in the center that fit the flux chamber and dipped approximately three cm below the water surface when floating in the stream.

A flux chamber was installed semi-permanently 16 m downstream of the peatland outlet for the duration of the study. A second flux chamber was installed 140 m downstream from the peatland outlet for 1.5 d between July 12th and July 14th before a large storm permanently damaged the sampling setup. Flux chambers collected data continuously at 15-min intervals. During synoptic sampling, the second flux chamber was used to collect measurements throughout the stream. CO_2 evasion measurements were collected at each site at 5-min measurement intervals for a total of 15 min per site. We used an average of the three evasion measurements in our calculations.

A discharge–water-level rating curve was developed by modeling the relationship between water-level and 40 discharge measurements collected over the course of the study period. We installed a water-level sensor (Model 3001, Solinst) 56 m from the outlet and programmed to collect measurements at 15-min intervals. Discharge measurements were collected using velocity profiling with a water velocity probe (Model FP101, Global Flow Probe, Global Water).

Results

Environmental observations

Over the five-week study period, our study site received 340 mm of rainfall (Appendix S1: Fig. S1). During this time, the maximum daily rainfall of 38.2 mm occurred on July 12th and was the largest daily rainfall event recorded at this site since records started in 2012. Average discharge was 8.57 L/s and average daily discharge ranged from 2.2 L/s to 64.82 L/s (Fig. 3). Average maximum daily discharge was 14.11 L/s. Average daily air temperature was 2.9°C, with a maximum single-day average of 5.5°C and a minimum single-day average of 1.4°C. The average stream temperature recorded was 6.5°C and daily averages ranged from 4.7°C to 8.7°C.

Continuous observations

$k_{600\text{-K}}$ values ranged from 5.24 to 62.3 m/d, with a mean of 15.6 ± 14.5 m/d and median 9.23 m/d. $k_{600\text{-M}}$ values collected during the same period ranged from 4.17 to 63.0 m/d, with a mean of 20.0 ± 6.20 m/d and median 18.6 m/d (Fig. 3). Using a linear regression model, we found a statistically significant relationship between discharge and $k_{600\text{-K}}$ ($P < 0.001$, $r^2 = 0.80$), between discharge and $k_{600\text{-M}}$ ($P < 0.001$, $r^2 = 0.38$), and between $k_{600\text{-M}}$ and CO_2 evasion ($P < 0.001$, $r^2 = 0.15$). While statistically significant, the relationship between discharge and $k_{600\text{-M}}$ did not always appear linear, particularly with regards to ~18 midrange $k_{600\text{-M}}$ measurements representing 15-min time segments collected at very high discharge (Fig. 3B). Downstream from the peatland outlet (140 m), similar trends were observed during the short period of observations. $k_{600\text{-M}}$ was positively correlated with both discharge ($P < 0.001$, $r^2 = 0.77$) and CO_2 evasion ($P < 0.001$, $r^2 = 0.99$), ranging from 0.076 to 40.0 m/d (Appendix S1: Fig. S2).

Variables measured throughout the course of this study showed diel variability, with daily maxima and minima occurring at different times of the day (Fig. 4). Based on 34 full days of data collection, we observed that daily minima for $k_{600\text{-M}}$, pCO_2, CO_2 evasion, and discharge occurred between 1300 and 1800 LT. Daily maxima for $k_{600\text{-M}}$ did not exhibit a clear pattern, though maxima were generally concentrated in the daytime hours. Daily maxima for pCO_2 and CO_2 evasion occurred in the hours prior to or immediately after sunrise, whereas daily maxima for discharge occurred in the afternoon and before sunset (Table 1).

Discrete observations

Slopes of measured sections within the study-reach averaged 8.6% and ranged from 0.04% to 20%. Average discharge on synoptic sampling days ranged from 8.18 L/s to 23.6 L/s. Overall $k_{600\text{-K}}$ values ranged from 0 to 515 m/d with a mean of 91.96 m/d along the stream (Fig. 5A). Mean values for a location ranged from 0.47 ± 0.51 m/d to 220.4 ± 97.6 m/d. We found a significant difference in values by location

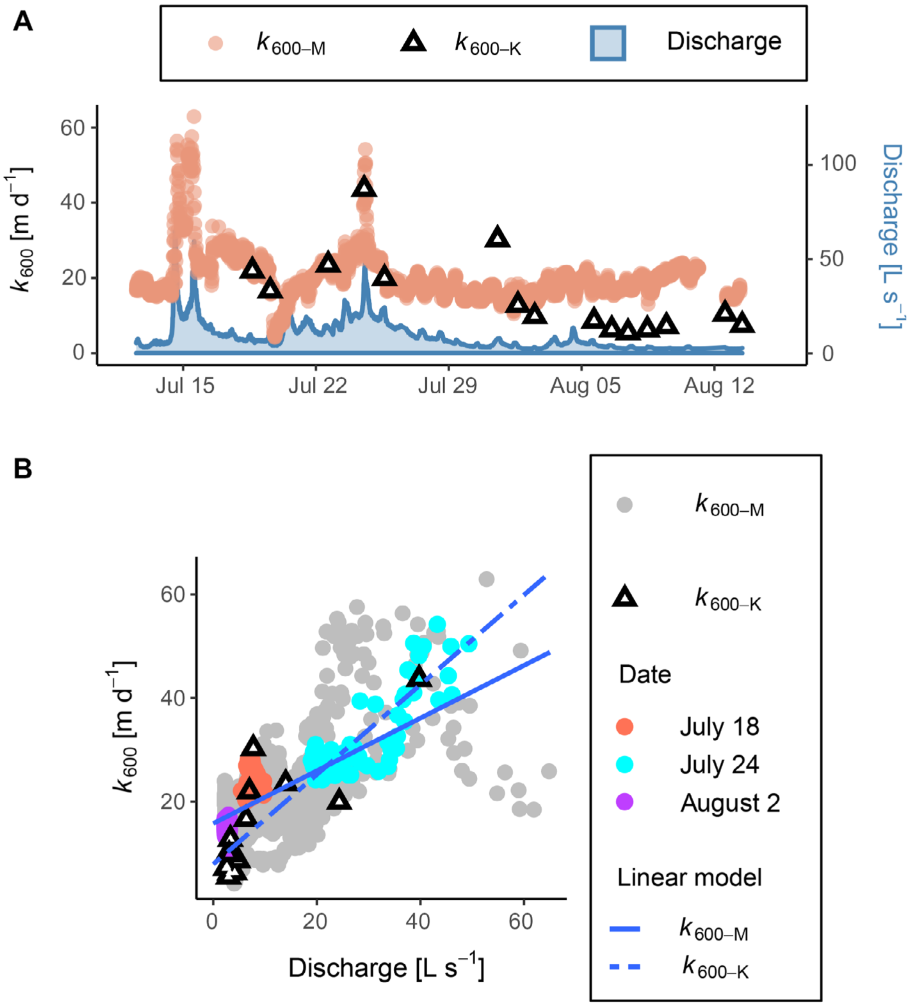

Fig. 3. (A) $k_{600\text{-M}}$ and $k_{600\text{-K}}$ values collected at a stationary location near the peatland outlet from 10 July 2019 to 18 August 2019. Discharge (L/s) is also shown. (B) $k_{600\text{-M}}$ (dots) and $k_{600\text{-K}}$ (triangles) values plotted by discharge collected every 15 min near the wetland outlet from 10 July 2019 to 18 August 2019. Measurements collected throughout three different days are highlighted. Days were selected to illustrate 24-h observations under low, medium, and high discharge. Linear regression models show the relationship between discharge and $k_{600\text{-M}}$ (solid) and $k_{600\text{-K}}$ (dashed).

($P < 0.001$). A post hoc multiple comparison test found 16 out of 561 site comparisons to be significant using the Bonferroni test for multiple comparison.

$k_{600\text{-M}}$ was calculated at 10 locations along the stream reach every 6–7 d. Values ranged from 6.5 to 444.4 m/d with a mean of 88.6 m/d (Fig. 5B). Average mean values for each sample location ranged from 22.5 ± 11.6 to 151.4 ± 167 m/d. We found a significant difference between dates of collection ($P = 0.03$), and a test for multiple comparison found a significant difference between two sample sites, at 94.1 m and 169.9 m from the wetland outlet.

$k_{600\text{-K}}$ and $k_{600\text{-M}}$ values collected over all synoptic campaigns were compared to one another by date of collection (Fig. 6). Note that only sites with co-located CO_2 evasion measurements were used in this comparison. $k_{600\text{-K}}$ values ranged from 67.2 ± 57.8 on August 13th to 131.2 ± 100.4 m/d on July 26th. $k_{600\text{-M}}$ values ranged from 68.9 ± 48.8 on August 1st to

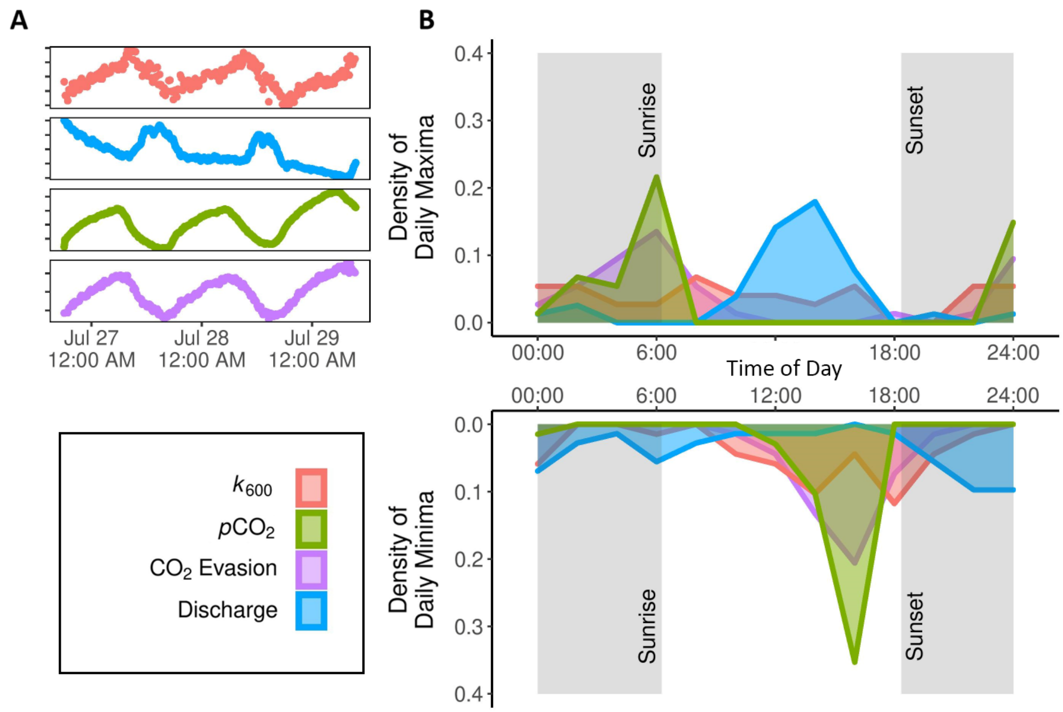

Fig. 4. (A) $k_{600\text{-M}}$ and discharge collected between July 26 at 10:00 AM and July 29 at 2:00 PM showing daily variation in $k_{600\text{-M}}$, Discharge, CO_2 flux, and dissolved CO_2, at low flows. (B) Maximum and minimum occurrence per day of CO_2 evasion, K600, Discharge, and dissolved CO_2 collected from July 13th to August 12th 2019.

Table 1. Time of day for daily minima and maxima for measured variables.

Variable	75th percentile occurrence of daily minimum	75th percentile occurrence of daily maximum
$k_{600\text{-M}}$	1:11 PM to 5:50 PM	4:04 AM to 3:11 PM
pCO_2	3:00 PM to 4:30 PM	4:42 AM to 7:14 AM
CO_2 evasion	2:53 PM to 5:15 PM	4:11 AM to 07:39 AM
Discharge	12:50 AM to 2:45 AM	12:04 PM to 2:37 PM
Temperature	6:56 AM to 7:30 AM	2:15 PM to 4:15 PM

121.4 ± 126.8 m/d on July 19th. Pairwise comparisons of each synoptic campaign revealed no statistically significant differences between methods (P values ranged from 0.22 to 0.97; Fig. 6).

Discussion

What were the observed ranges of gas transfer velocity in a páramo stream?

Using two independent methods to evaluate spatial variation in k_{600}, we found that $k_{600\text{-K}}$ values measured along a 250-m study reach ranged from 0 to 515 m/d (mean = 91.9 ± 89.9 m/d), whereas $k_{600\text{-M}}$ values ranged from 6.5 to 444 m/d (mean = 88.6 ± 73.2 m/d). Continuous measurements of $k_{600\text{-M}}$ collected near the peatland outlet fell within these ranges. In general, these measurements were in good agreement with k values reported by previous studies in mountainous and steep streams conducted through various techniques, including argon injections in the Swiss Alps (8.1–4118, mean = 464 m/d; Ulseth et al. 2019), argon injections in the Rocky Mountains (5.6–208, mean = 56.3 m/d; Hall and Madinger 2018), CO_2 injections in British Columbia (15.1–237, mean = 58.4 m/d; McDowell and Johnson 2018), SF_4 injections in the UK (2.6–296, mean = 55.1 m/d; Maurice et al. 2017), and propane injections in the Austrian Alps (2.9–177, mean = 30.0 m/d; Schelker et al. 2016; Appendix S1: Fig. S2). On average, however, our study reports higher k_{600} values than most studies previously referenced with the exception of those reported by Ulseth et al. (2019).

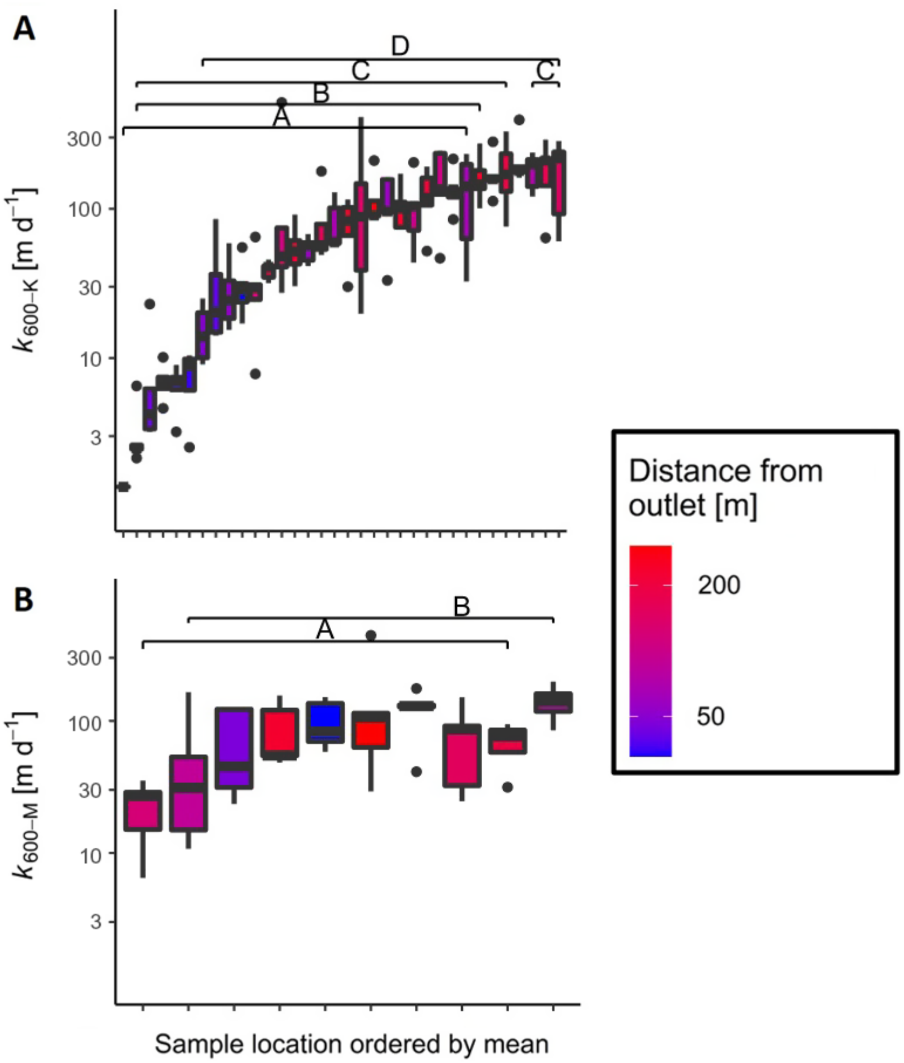

Fig. 5. (A) Distribution of $k_{600\text{-K}}$ values by synoptic sample location, arranged by mean value and colored by distance from wetland outlet. Significant differences between locations are shown. (B) Distribution of $k_{600\text{-M}}$ values by synoptic sample location, arranged by mean value, and colored by distance from wetland outlet.

Analysis of the physical characteristics of páramo streams offers insight into the potential drivers behind differences in k_{600} observations in our study in relation to those of previous studies. On average, velocity measurements were at least two times greater in our study than in previous studies (Appendix S1: Fig. S3). Average slopes in our study were steeper in four out of the five reported studies, whereas channel width was much narrower in our study than those previous studies. Velocity and slope are major factors driving stream turbulence and therefore gas transfer (Raymond et al. 2012, Long et al. 2015), whereas smaller hydraulic diameters, including channel width, have been linked to higher k_{600} values (Kokic et al. 2018). These differences highlight the influence of stream morphology on k_{600} and offer a likely explanation for the higher $k_{600\text{-M}}$ observed in our study. An exception to this pattern was the range of k_{600} values of Ulseth et al. (2019), where velocity and slope were quite similar to our study (within 15% and 1.0% difference, respectively), but discharge was much greater than in our study and likely the reason for the

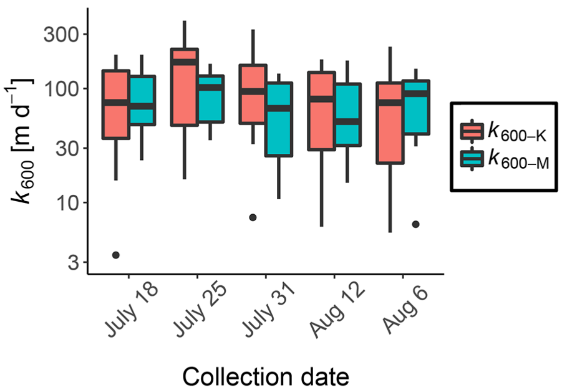

Fig. 6. Boxplots show $k_{600\text{-M}}$ and $k_{600\text{-K}}$ values by collection date, sampled at 10 locations on five different days, and colored by average discharge readings taken throughout the collection period.

difference in k. A positive relationship between discharge and k reported here has also been observed elsewhere (Billett and Harvey 2013, McDowell and Johnson 2018, Ulseth et al. 2019).

While not measured in this study, streambed roughness may also be responsible for observed differences in k. Our study stream carved through a deep peatland and upland soils and was almost entirely absent of rocks and woody debris. Ulseth et al. (2019) found a strong positive relationship between stream bed roughness and k. Friction between stream water and benthic substrate creates turbulence that leads to higher k, a process that is particularly pronounced in small streams (Kokic et al. 2018). This suggests that aquatic environments dominated by rocky substrates, such as streams in temperate regions with thin soils, could have higher turbulence than smooth substrate in the páramo at similar velocities.

Finally, differences in methodology used to estimate k may also be contributing to the discrepancy in the reported values. We evaluate k throughout a 250-m reach, whereas studies that use tracer methods integrate k over the length of the injection reach. Nonetheless, there may be weaknesses in both methods that should be considered when interpreting k estimates. Our method provides a characterization of k at individual points along a stream and at high temporal resolutions; however, if the geomorphology of the stream is not equally characterized, k estimates lack context for interpretation. Flux chambers cannot measure evasion from disjointed stream segments such as waterfalls. On the other hand, argon, propane, and SF_4 tracer methods have limitations in highly turbulent streams where turbulent-diffusive exchange may switch to bubble-mediated exchange. Bubble-mediated exchange, which occurs at high turbulence, is mass-dependent and affects gasses differently, complicating scaling from one gas to another (Hall and Madinger 2018, Ulseth et al. 2019). Direct comparison of two or more methods is needed to fully evaluate the difference between a chamber-based method like the one used here and more common tracer methods. Taken together, our findings suggest that despite relatively low discharge, the incised and narrow, high-velocity streams typical of the páramo exhibit quite high gas transfer velocities. Furthermore, our estimates of k remain conservative, as they do not account for the large waterfall in the middle of the study reach. Further characterization of k is critical to accurately quantify CO_2 evasion from mountain rivers. Developing an empirical relationship between k and discharge may be a useful first step.

How does gas transfer velocity vary at small spatial scales?

Using both methods for deriving k_{600}, we found significant spatial heterogeneity of k_{600} values within the relatively short 250-m stream reach. Measurements of k_{600} collected on multiple days during the study period were found to vary greatly from location to location (<10 m; Fig. 5). Variance of k_{600} for a single location was also evident as measurements could vary by orders of magnitude from day to day (Fig. 5). However, our sample size was small and increased sampling of these sites may reveal more robust statistical differences. Our finding, however, is in line with previous observations that suggest the geomorphology of headwater streams, alternating between riffles, pools, and waterfalls, results in points along the stream that drive disproportionally greater CO_2 evasion (Wallin et al. 2011, Billett and Harvey 2013, Rocher-Ros et al. 2019).

The high spatial resolution of k_{600} values in this study and their relationship to the physical characteristics found in small páramo streams are likely responsible for the high spatial variability in CO_2 evasion. In fact, $k_{600\text{-M}}$ and CO_2 evasion are positively correlated ($P < 0.05$, $r^2 = 0.113$). While for this same stream Schneider et al. (2020) showed that pCO_2 and CO_2 evasion were higher near the peatland outlet and progressively decreased downstream, k_{600} did not follow a clear longitudinal pattern. Instead, measurements collected over the five synoptic campaigns suggest that stream channel morphology mediates the spatial variability of gas transfer velocities in páramo streams. Future studies should expand upon these relationships, account for the limitations imposed by local C availability, and apply these concepts across streams of varying sizes and morphologies in complex terrain.

How does gas transfer velocity vary in response to rain events and during more stable conditions?

We observed a strongly positive response of k_{600} to rapid increases in discharge following large rain events. This positive response was consistent for upstream (Fig. 3) and downstream (Appendix S1: Fig. S2) locations, although downstream observations were considerably shorter in duration due to sensor damage. While $k_{600\text{-M}}$ increases during storm events were pronounced, they were short-lived and usually lasted less than 24 h. Previous studies reported a strong relationship between k and discharge in steep-sloped, headwater streams (Billett and Harvey 2013, Natchimuthu et al. 2017, McDowell and Johnson 2018). Rainfall has been found to be an important, though often overlooked factor influencing k_{600} (Guérin et al. 2007). As discharge increases so do velocity and turbulence, but the relationship is site-specific and dependent on the geomorphology of the stream (Hall and Madinger 2018, Ulseth et al. 2019). In our study, discharge explained only 38% of $k_{600\text{-M}}$ variation collected continuously throughout the study period, and a linear regression often overpredicted $k_{600\text{-M}}$ at very high discharges (Fig. 3). Outliers suggest that the relationship between discharge and k_{600} may not be linear, an unexpected finding that may not be unique to our study (Genzoli and Hall 2016). Further exploration of this relationship would require additional sampling at shorter intervals as only two sensors may not fully capture rapid changes in the system. Increasing sample locations while reducing sampling intervals would allow for a comprehensive evaluation of relationship between storm-driven discharge and k_{600}.

It is also important to note that the majority of k_{600} values recorded in this study were not influenced by storm-driven discharge. Ninety percent of $k_{600\text{-M}}$ values collected near the peatland outlet were between 14.0 and 28.9 m/d, less than half of the maximum value recorded. When not influenced by large rain events, smaller levels of variance in $k_{600\text{-M}}$ seemed to occur on a diel basis (Fig. 4). Furthermore, daily maxima and daily minima occurred at predictable times throughout the day for most variables, including pCO_2, CO_2 evasion, and discharge. Patterns in the diel cycling of pCO_2 and CO_2 evasion may be influenced by sunlight and primary production and respiration taking place in the peatland, as observed in other aquatic environments (Abril et al. 2014, Riveros-Iregui et al. 2018, Rocher-Ros et al. 2019). Patterns of CO_2 evasion closely mirrored pCO_2 concentrations, suggesting that pCO_2 is a driver of CO_2 evasion throughout the day. Discharge peaked in early afternoon and minima occurred in the early morning, likely as a result of diurnal melting and nocturnal freezing occurring at higher elevation (Jacobsen et al. 2014). We observed a clear pattern of daily minima of $k_{600\text{-M}}$ in the afternoon, which coincided with daily minima of CO_2 evasion (Fig. 4). On the other hand, daily maxima of $k_{600\text{-M}}$ were less clear, likely because the combined effects of pCO_2, CO_2 evasion, and discharge dynamics throughout the day.

Our method for calculating $k_{600\text{-M}}$ allows for what may be the first high-resolution assessment of k_{600} values over time, showing k_{600} to exhibit diurnal cycles broken by abrupt spikes due to increasing discharge. k_{600} response to storm events is an important contribution to our current understanding of gas transfer velocity and suggests that storm events may drive considerable pulses in CO_2 evasion. These findings highlight the significant relationship between precipitation and k_{600}, suggesting rainfall may be used as a first-degree predictor of the temporal variability of k_{600}. Nonetheless, during more stable conditions, other factors such as concentration of dissolved CO_2 or CO_2 evasion may also influence diel trends in k_{600}.

How did the two independent methods used for calculating k_{600} compare to one another?

Our results suggest that the two independent methods to estimate k_{600} were in good agreement at high discharge, but $k_{600\text{-K}}$ was consistently lower than $k_{600\text{-M}}$ at low discharge (Fig. 3). The two independent methods used to calculate k_{600} were similar in range and relationship to discharge. Comparison of aggregated synoptic sampling by date did not find a significant difference between methods (Fig. 6). The agreement between methods adds confidence to the accuracy of k_{600} provided in this study. However, the discrepancy between methods at low discharge may be a result of difference in the geomorphological properties of our streams compared to those used to derive the empirical equation for $k_{600\text{-K}}$ proposed by Raymond et al. (2012). This equation was developed from an extensive database of North American streams. Although all streams were relatively small (discharge ranged 2.83–209,420, median 546 L/s), our stream would fall among the smallest in their data set (median discharge, 4.19 L/s). In contrast, average velocity collected in our stream (median velocity 0.103 m/s) is much higher relative to average discharge, and these two parameters deviate from the empirical discharge-velocity regression found by Raymond et al. (2012; velocity range 0.0064–1.21, median 0.135 m/s). Thus, páramo streams may not be well represented by the equation used to calculate $k_{600\text{-K}}$, likely due to differences in the terrain and the emerging hydraulic relationships between discharge and velocity. Raymond et al. (2012) noted the need for increased measurements of high-velocity, steep streams to improve model accuracy as well as the role of streambed roughness, a characteristic that is likely to differ between North American and páramo streams. The compatibility of differing methods for determining k_{600} has important implications for further research of CO_2 evasion in tropical, mountainous environments such as the páramo. Measurements needed to calculate $k_{600\text{-K}}$ are easily and rapidly collected, requiring minimal instrumentation. However, our results suggest that such methods could be limited in their ability to characterize temporal variation of k at a single site. Measurements needed to calculate $k_{600\text{-M}}$ require equipment that once deployed at one site, may not always be well-suited to high velocity, turbulent waters. However, our $k_{600\text{-M}}$ method was able to capture variation of k_{600} through periods of rapidly changing discharge. Taken together, our findings suggest that both methods are valuable in the characterization of k_{600} across a heterogeneous stream and used in tandem could offer a way to overcome their individual limitations. Future pairing of $k_{600\text{-K}}$ and $k_{600\text{-M}}$ measurements could yield empirical relationships better suited for the hydraulic properties of not only páramo environments but also other mountainous streams. Regardless, additional methods for assessing k_{600} are needed for a more complete analysis of k_{600} that includes extremely turbulent areas such as waterfalls.

Conclusion

Our study provides a high-resolution assessment of k_{600} in a high-elevation tropical catchment across steep environmental gradients and highlights the combined effects of hydrology and stream morphology in co-regulating gas transfer velocities in páramo streams. We observed variability of gas transfer velocities within short time scales and across short distances. Our findings suggest that increased discharge following rain events is a major control on the temporal variability of k_{600}. Independent methods used for calculating k_{600} are in good agreement at high and medium discharge levels, but $k_{600\text{-K}}$ seems to underestimate $k_{600\text{-M}}$ at low discharge. Findings from this study indicate that variability in k_{600} values could be missed if the full geomorphology and the range of environmental conditions of a site are not considered, particularly in mountainous terrain. Additional observations may provide insight into the relationship between k_{600}, the physical properties of the stream, and the magnitude and timing of precipitation in páramo ecosystems. Our findings offer parameterization of a variable critical to estimating greenhouse gas emissions from aquatic environments in an important yet understudied ecosystem. As such, this study is an important step toward improving the accuracy of the C budgets in mountainous environments.

Acknowledgments

K. M. Whitmore and N. Stewart contributed equally to the work reported here. This work was supported by the U.S. National Science Foundation grant # EAR-1847331. We would like to thank the staff at the University of San Francisco Quito (USFQ) for logistical support as well as the communities of Cumbayá and Quito, Ecuador. Gonzalo Rivas-Torres provided drone imagery for slope calculations. We thank the Ministry of the Environment of Ecuador (research permit # 014-018-IC-FLO-DPAN/MA) and the National System of Protected Areas of Ecuador for site access. Two anonymous reviewers and the handling editor provided valuable feedback in a previous version of this manuscript.

Literature Cited

Abril, G., et al. 2014. Amazon River carbon dioxide outgassing fuelled by wetlands. Nature 505:395–398.

Aufdenkampe, A. K., E. Mayorga, P. A. Raymond, J. M. Melack, S. C. Doney, S. R. Alin, R. E. Aalto, and K. Yoo. 2011. Riverine coupling of biogeochemical cycles between land, oceans, and atmosphere. Frontiers in Ecology and the Environment 9:53–60.

Battin, T. J., S. Luyssaert, L. A. Kaplan, A. K. Aufdenkampe, A. Richter, and L. J. Tranvik. 2009. The boundless carbon cycle. Nature Geoscience 2:598–600.

Benstead, J. P., and D. S. Leigh. 2012. An expanded role for river networks. Nature Geoscience 5:678–679.

Billett, M. F., and F. H. Harvey. 2013. Measurements of CO_2 and CH_4 evasion from UK peatland headwater streams. Biogeochemistry 114:165–181.

Bott, T. L. 2007. CHAPTER 28 - Primary productivity and community respiration. Pages 663–690 *in* F. R. Hauer, and G. A. Lamberti, editors. Methods in stream ecology. Second edition. Academic Press, San Diego, California, USA.

Butman, D., and P. A. Raymond. 2011. Significant efflux of carbon dioxide from streams and rivers in the United States. Nature Geoscience 4:839–842.

Campeau, A., K. H. Bishop, M. F. Billett, M. H. Garnett, H. Laudon, J. A. Leach, M. B. Nilsson, M. G. Öquist, and M. B. Wallin. 2017. Aquatic export of young dissolved and gaseous carbon from a pristine boreal fen: implications for peat carbon stock stability. Global Change Biology 23:5523–5536.

Cole, J. J., et al. 2007. Plumbing the global carbon cycle: integrating inland waters into the terrestrial carbon budget. Ecosystems 10:172–185.

Crawford, J. T., R. G. Striegl, K. P. Wickland, M. M. Dornblaser, and E. H. Stanley. 2013. Emissions of carbon dioxide and methane from a headwater stream network of interior Alaska. Journal of Geophysical Research: Biogeosciences 118:482–494.

Downing, J. A., J. J. Cole, C. M. Duarte, J. J. Middelburg, J. M. Melack, Y. T. Prairie, P. Kortelainen, R. G. Striegl, W. H. McDowell, and L. J. Tranvik. 2012. Global abundance and size distribution of streams and rivers. Inland Waters 2:229–236.

Food and Agriculture Organization of the United Nations, editor. 2003. Review of world water resources by country. Food and Agriculture Organization of the United Nations, Rome, Italy.

Genzoli, L., and R. O. Hall. 2016. Shifts in Klamath River metabolism following a reservoir cyanobacterial bloom. Freshwater Science 35:795–809.

Guérin, F., G. Abril, D. Serça, C. Delon, S. Richard, R. Delmas, A. Tremblay, and L. Varfalvy. 2007. Gas transfer velocities of CO_2 and CH_4 in a tropical reservoir and its river downstream. Journal of Marine Systems 66:161–172.

Hall, R. O. Jr, and H. L. Madinger. 2018. Use of argon to measure gas exchange in turbulent mountain streams. Biogeosciences 15:3085–3092.

Horgby, A., P. L. Segatto, E. Bertuzzo, R. Lauerwald, B. Lehner, A. J. Ulseth, T. W. Vennemann, and T. J. Battin. 2019. Unexpected large evasion fluxes of carbon dioxide from turbulent streams draining the world's mountains. Nature Communications 10:1–9.

Hotchkiss, E. R., R. O. Jr Hall, R. A. Sponseller, D. Butman, J. Klaminder, H. Laudon, M. Rosvall, and J. Karlsson. 2015. Sources of and processes controlling CO_2 emissions change with the size of streams and rivers. Nature Geoscience 8:696–699.

Hribljan, J. A., E. Suarez, L. Bourgeau-Chavez, S. Endres, E. A. Lilleskov, S. Chimbolema, C. Wayson, E. Serocki, and R. A. Chimner. 2017. Multidate, multisensor remote sensing reveals high density of carbon-rich mountain peatlands in the páramo of Ecuador. Global Change Biology 23:5412–5425.

Jacobsen, D., P. Andino, R. Calvez, S. Cauvy-Fraunié, R. Espinosa, and O. Dangles. 2014. Temporal variability in discharge and benthic macroinvertebrate assemblages in a tropical glacier-fed stream. Freshwater Science 33:32–45.

Jähne, B., G. Heinz, and W. Dietrich. 1987. Measurement of the diffusion coefficients of sparingly soluble gases in water. Journal of Geophysical Research: Oceans 92:10767–10776.

Johnson, M. S., M. F. Billett, K. J. Dinsmore, M. Wallin, K. E. Dyson, and R. S. Jassal. 2010. Direct and continuous measurement of dissolved carbon dioxide in freshwater aquatic systems—method and applications. Ecohydrology 3:68–78.

Johnson, M. S., J. Lehmann, S. J. Riha, A. V. Krusche, J. E. Richey, J. P. H. Ometto, and E. G. Couto. 2008. CO_2 efflux from Amazonian headwater streams represents a significant fate for deep soil respiration. Geophysical Research Letters 35:L17401.

Josse, C., F. Cuesta, G. Navarro, V. Barrena, E. Cabrera, E. Chacón-Moreno, W. Ferreira, M. Peralvo, J. Saito, and A. Tovar. 2009. Ecosistemas de los Andes del Norte y Centro. Bolivia, Colombia, Ecuador, Perú y Venezuela. Secretaría General de la Comunidad Andina, Programa Regional ECOBONA-Intercooperation, CONDESAN-Proyecto Páramo Andino, Programa BioAndes, EcoCiencia, NatureServe, IAvH, LTA-UNALM, ICAE-ULA, CDC-UNALM, RUMBOL SRL., Lima, Perú.

Kokic, J., E. Sahlée, S. Sobek, D. Vachon, and M. B. Wallin. 2018. High spatial variability of gas transfer velocity in streams revealed by turbulence measurements. Inland Waters 8:461–473.

Lauerwald, R., G. G. Laruelle, J. Hartmann, P. Ciais, and P. A. Regnier. 2015. Spatial patterns in CO_2 evasion from the global river network. Global Biogeochemical Cycles 29:534–554.

Long, H., L. Vihermaa, S. Waldron, T. Hoey, S. Quemin, and J. Newton. 2015. Hydraulics are a first-order control on CO_2 efflux from fluvial systems. Journal of Geophysical Research: Biogeosciences 120:1912–1922.

Marzolf, E. R., P. J. Mulholland, and A. D. Steinman. 1994. Improvements to the diurnal upstream–downstream dissolved oxygen change technique for determining whole-stream metabolism in small streams. Canadian Journal of Fisheries and Aquatic Sciences 51:1591–1599.

Maurice, L., B. G. Rawlins, G. Farr, R. Bell, and D. C. Gooddy. 2017. The influence of flow and bed slope on gas transfer in steep streams and their implications for evasion of CO_2. Journal of Geophysical Research: Biogeosciences 122:2862–2875.

McCutchan, J. H., W. M. Lewis, and J. F. Saunders. 1998. Uncertainty in the estimation of stream metabolism from open-channel oxygen concentrations. Journal of the North American Benthological Society 17:155–164.

McDowell, M. J., and M. S. Johnson. 2018. Gas transfer velocities evaluated using carbon dioxide as a tracer show high streamflow to be a major driver of total CO_2 evasion flux for a headwater stream. Journal of Geophysical Research: Biogeosciences 123:2183–2197.

Mena Vásconez, P., and G. Medina. 2001. La biodiversidad de los páramos en el Ecuador. Los Páramos de Ecuador. Particularidades, Problemas y Perspectivas. Pages 27–52. Editorial Abya Yala, Quito.

Natchimuthu, S., M. B. Wallin, L. Klemedtsson, and D. Bastviken. 2017. Spatio-temporal patterns of stream methane and carbon dioxide emissions in a hemiboreal catchment in Southwest Sweden. Scientific Reports 7:39729.

NOAA ESRL Global Monitoring Laboratory. 2019. Atmospheric carbon dioxide dry air mole fractions from quasi-continuous measurements at Mauna Loa, Hawaii, Barrow, Alaska, American Samoa and South Pole. Version 2020-04. National Oceanic and Atmospheric Administration (NOAA), Earth System Research Laboratories (ESRL), Global Monitoring Laboratory (GML), Boulder, Colorado, USA. https://doi.org/10.15138/yaf1-bk21

Raymond, P. A., et al. 2013. Global carbon dioxide emissions from inland waters. Nature 503:355–359.

Raymond, P. A., C. J. Zappa, D. Butman, T. L. Bott, J. Potter, P. Mulholland, A. E. Laursen, W. H. McDowell, and D. Newbold. 2012. Scaling the gas transfer velocity and hydraulic geometry in streams and small rivers. Limnology and Oceanography: Fluids and Environments 2:41–53.

Riveros-Iregui, D. A., T. P. Covino, and R. González-Pinzón. 2018. The importance of and need for rapid hydrologic assessments in Latin America. Hydrological Processes 32:2441–2451.

Rocher-Ros, G., R. A. Sponseller, W. Lidberg, C.-M. Mörth, and R. Giesler. 2019. Landscape process domains drive patterns of CO_2 evasion from river networks. Limnology and Oceanography Letters 4:87–95.

Sánchez, M. E., R. A. Chimner, J. A. Hribljan, E. A. Lilleskov, and E. Suárez. 2017. Carbon dioxide and methane fluxes in grazed and undisturbed mountain peatlands in the Ecuadorian Andes. Mires and Peat 19:1–18.

Schelker, J., G. A. Singer, A. J. Ulseth, S. Hengsberger, and T. J. Battin. 2016. CO_2 evasion from a steep, high gradient stream network: importance of seasonal and diurnal variation in aquatic pCO_2 and gas transfer. Limnology and Oceanography 61:1826–1838.

Schneider, C. L., M. Herrera, M. L. Raisle, A. R. Murray, K. M. Whitmore, A. C. Encalada, E. Suárez, and D. A. Riveros-Iregui. 2020. Carbon dioxide (CO_2) fluxes from terrestrial and aquatic environments in a high-altitude tropical catchment. Journal of Geophysical Research: Biogeosciences 125: e2020JG005844.

Sklenář, P., and S. Lægaard. 2003. Rain-shadow in the high Andes of Ecuador evidenced by paramo vegetation. Arctic, Antarctic, and Alpine Research 35:8–17.

Tix, J. A., C. T. Hasler, C. Sullivan, J. D. Jeffrey, and C. D. Suski. 2017. Elevated carbon dioxide has limited acute effects on *Lepomis macrochirus* behaviour. Journal of Fish Biology 90:751–772.

Ulseth, A. J., R. O. Hall, M. Boix Canadell, H. L. Madinger, A. Niayifar, and T. J. Battin. 2019. Distinct air–water gas exchange regimes in low- and high-energy streams. Nature Geoscience 12:259–263.

Wallin, M. B., M. G. Öquist, I. Buffam, M. F. Billett, J. Nisell, and K. H. Bishop. 2011. Spatiotemporal variability of the gas transfer coefficient (KCO_2) in boreal streams: implications for large scale estimates of CO_2 evasion. Global Biogeochemical Cycles 25. https://doi.org/10.1029/2010GB003975

Wanninkhof, R. 2014. Relationship between wind speed and gas exchange over the ocean revisited. Limnology and Oceanography: Methods 12:351–362.

Zappa, C. J., W. R. McGillis, P. A. Raymond, J. B. Edson, E. J. Hintsa, H. J. Zemmelink, J. W. Dacey, and D. T. Ho. 2007. Environmental turbulent mixing controls on air-water gas exchange in marine and aquatic systems. Geophysical Research Letters 34. https://doi.org/10.1029/2006GL028790

Data Availability

Data and code are available from the University of North Carolina Digital Repository: https://doi.org/10.17615/zyrb-9916.

Supporting Information

Additional Supporting Information may be found online at: http://onlinelibrary.wiley.com/doi/10.1002/ecs2.3647/full